

# Enceladus' Water Vapor Plume

Candice J. Hansen<sup>1\*</sup>, L. Esposito<sup>2</sup>, A. I. F. Stewart<sup>2</sup>, J. Colwell<sup>2</sup>, A. Hendrix<sup>1</sup>, W. Pryor<sup>4</sup>,  
D. Shemansky<sup>3</sup>, R. West<sup>1</sup>

<sup>1</sup>Jet Propulsion Laboratory / California Institute of Technology

\* To whom correspondence should be addressed

Mail Stop 169-237

4800 Oak Grove Dr.

Pasadena, CA 91109-8099

818-354-7675

Candice.j.Hansen@jpl.nasa.gov

<sup>2</sup>Laboratory for Air and Space Physics (LASP), University of Colorado, Boulder, CO

<sup>3</sup>University of Southern California

<sup>4</sup>Central Arizona College

Submitted to Science October 11, 2005

Re-submitted to Science December 22, 2005; final submission January 18, 2006

## **Abstract**

**The Cassini spacecraft flew close to Saturn's small moon, Enceladus, three times in 2005. Cassini's UltraViolet Imaging Spectrograph observed stellar occultations on two flybys and confirmed the existence, composition and regionally confined nature of a water vapor plume in the south polar region of Enceladus. The plume supplies an adequate amount of water to re-supply the E ring against losses and to be the dominant source of the neutral OH and atomic oxygen that fill the Saturnian system.**

The youthful geologic appearance of Enceladus (1) and the correlation of the E ring peak density with the orbit of Enceladus (2) have long led scientists to speculate that Enceladus is the source of Saturn's E ring (2-5). The narrow size distribution of particles in the E ring suggests a liquid or vapor origin, in contrast to the broad range of particle sizes that would be generated by impacts (2). To test the hypothesis that Enceladus has geologic activity supplying the E ring and neutral species in Saturn's magnetosphere the Cassini UltraViolet Imaging Spectrograph (UVIS) team planned stellar occultation observations on the first and third close flybys of Enceladus to search for the presence of a tenuous atmosphere (6). The detection, by the Cassini Magnetometer team (7), of draped field lines consistent with the presence of an atmosphere gave further impetus to the second occultation observation. Because of Enceladus' small size and weak gravity ( $\sim 12 \text{ cm/sec}^2$ ) any sputtered or sublimated atmosphere will be lost (8); thus if a tenuous atmosphere were to be detected it would have to come from some sort of geologic

activity. We now know that this is the case and we report here on the results established by the occultations observed by UVIS.

Observations of stellar occultations are a sensitive method for looking for the presence of tenuous atmospheres (9), particularly at ultraviolet wavelengths where many gases have strong absorptions. The Cassini UVIS has 4 optical channels: the High Speed Photometer (HSP), the Extreme UltraViolet (EUV) spectrograph, the Far UltraViolet (FUV) spectrograph, and the Hydrogen/Deuterium Absorption Cell (6). The HSP and FUV were used to observe the occultations. The HSP is sensitive to 1100 to 1900 Å and is read out once per 2 msec. The FUV also covers the range 1100 Å to 1900 Å, and was configured with 512 spectral bins (1.56 Å resolution) for the July occultation observation. The FUV integration time was 5 sec.

The star lambda Scorpii (Shaula) was occulted by Enceladus on February 17, 2005, the first of three close Enceladus flybys (Figure 1.a). A second occultation, of the star gamma Orionis (Bellatrix), was observed on the third and closest flyby on July 14, 2005 (Fig. 1.b-d). Only the gamma Orionis ingress showed attenuation of starlight due to the presence of an absorbing gas. No detectable change of signal was detected by the HSP or FUV on the lambda Scorpii occultation before or after the star's signal was blocked by Enceladus. Detection and non-detections and ingress and egress locations are summarized in Table 1.

In the HSP and FUV data for the gamma Orionis occultation ingress, which occurred at  $-76^{\circ}$  latitude, the signal was attenuated as the star passed behind Enceladus' plume (Fig. 2). The starlight started to decrease at  $\sim 24$  sec prior to ingress, at a ray altitude of  $\sim 155$  km. The signal of the star was lost completely at UTC 19:54:56 when the star crossed behind the hard limb. The HSP has a finite recovery time on bright stars such as gamma Orionis, so it is not possible to separate a weak atmospheric signal from the instrument response on egress. For egress measurements we summed the FUV spectral pixels, but the temporal resolution is lower than the HSP data because of the longer integration time. No detectable change of signal was seen in FUV data on the egress of gamma Orionis. Clearly the gas detected at the ingress of the gamma Orionis occultation is not globally distributed. The data are consistent with a plume of gas over the southern pole.

The presence of an absorbing gas shows up in the FUV spectrum as relatively narrow features at short wavelengths and a broad shallow absorption from  $\sim 1450$  to  $1800 \text{ \AA}$  compared to the unocculted spectrum (Fig. 3). Time record 33, the last full 5 sec integration prior to ingress, shows the deepest absorption. The ray altitude above Enceladus' surface corresponding to time record 33 ranged from 30 to 7 km.

The average unocculted star spectrum ( $I_0$ ) was computed from 25 time records summed over 3 spatial rows (the instrument pointing drifted slightly over the course of the occultation). The ratio of time record 33 ( $I$ ) to  $I_0$  shows the spectrum of the absorbing gas (Fig. 4). We fit the spectrum to water by computing  $I = I_0 \exp(-n \cdot \sigma)$  for water, where  $\sigma$  is

the cross-section as a function of wavelength (10) and  $n$  is the column density. Figure 4 compares a water spectrum with column density  $n = 1.5 \times 10^{16} \text{ cm}^{-2}$  to the  $I/I_0$  spectrum for time record 33. This column density represents the integrated effect of water vapor along the ray path from the spacecraft to the star through the atmosphere. Statistical analysis of smoothed data shows that the water vapor absorption exceeds 2 sigma beginning with time record 29. The slight mismatch at short wavelengths may be due to using absorption cross-sections that were measured at room temperature (the absorption cross-sections at longer wavelengths which dominate our fit are not as affected by temperature (11)).

A significant molecule not apparent in the FUV absorption spectrum is CO. The Cassini Ion Neutral Mass Spectrometer detected a constituent with mass = 28 amu which could be  $\text{N}_2$  or CO (12). The Cassini UVIS observation however sets an upper limit of  $< 1.3 \times 10^{14} \text{ cm}^{-2}$  from the absence of CO A-X ( $v', 0$ ) absorption bands (13) at 1544, 1510, 1477, and 1447 Å assuming a 10% dip in the signal is required for positive identification of an absorption feature.

Looking at the slant column abundance of the water vapor vs. altitude (Fig. 5), the attenuation of the star signal during the gamma Orionis ingress is best fit with an exponential decline with altitude. The best fit scale length,  $L$ , is 80 km. (Since this is an escaping atmosphere this is not the same as the scale height for a gravitationally bound

atmosphere.) Time records 27 and 28 appear to show the presence of water, though not yet at a two sigma confidence level.

The loss rate of water from Enceladus,  $S$ , is given by the product of the molecular abundance,  $N$  ( $= n/h$ ), the plume area,  $h^2$ , and the velocity,  $v$ :

$$S = N * h^2 * v = n * h * v$$

We estimate the typical linear dimension of the plume,  $h$ , as the measured scale length,  $L = 80$  km. The observed column density along the path to the star is  $n = 1.5 \times 10^{16} \text{ cm}^{-2}$ .

If we assume the density corresponds to vapor in vapor pressure equilibrium with a warm ice source, then the temperature of the ice is  $\sim 145$  K. A lower limit for the velocity is the thermal velocity at  $T = 145$  K, which gives  $v = 41,200$  cm/sec. Note that  $v$  is well above the 24,000 cm/sec escape velocity. The flux is thus at least  $S = 5 \times 10^{27}$  molecules / sec.

With these simple assumptions the amount of water escaping from Enceladus is  $\sim 150$  kg/sec. Alternatively  $h$  can be estimated from the horizontal dimension of the plume crossed by the star during the course of the occultation,  $\sim 175$  km. Analysis by the Cassini Composite Infrared Spectrometer team of their thermal data indicates that temperatures could be as high as 180 K (14). At 180 K the thermal velocity  $v$  is 46,000 cm/sec. Using  $h = 175$  km and  $v = 46,000$  cm/sec, gives  $S > 1 \times 10^{28}$  molecule / sec, approximately 350 kg / sec.

Saturn's E ring, composed of water ice grains primarily 0.3 to 3 microns in size (15), extends from  $\sim 3$  to at least 8 Saturn radii with a peak density at Enceladus' orbit (2).

Analysis by Jurac *et al.*, 2001 (16) concluded that lifetimes of 1 micron grains are < 50 years because water molecules are sputtered from the grains' surfaces by the plasma trapped in Saturn's magnetosphere. A source of water is needed to maintain the E ring.

Saturn's system is filled with neutral products from the electron- and photo-dissociation of H<sub>2</sub>O molecules: Hubble Space Telescope observations detected neutral OH (17), and UVIS detected neutral atomic oxygen throughout Saturn's system (18). Most H<sub>2</sub>O molecules dissociate to H + OH, with more O coming from subsequent dissociation of OH. Neutrals are lost from the system due to charge exchange and collisions with ions. From measured O and OH abundances and theoretical estimates of loss processes of all water products from the system various investigators have estimated H<sub>2</sub>O supply rates necessary to maintain a steady state: >2 x 10<sup>27</sup> H<sub>2</sub>O / sec (17), possibly as high as 3.75 x 10<sup>27</sup> (19), or 10<sup>28</sup> H<sub>2</sub>O / sec (20, 21). Potential H<sub>2</sub>O sources identified previously by these investigators included sputtering and collisions, however rates of these processes are not sufficient to replace the lost neutrals (19). The inferred source rate of H<sub>2</sub>O in the present observations is of the same order as the earlier estimated loss rates for O and OH. If Enceladus is responsible for the majority of water product gas in the magnetosphere this implies more or less continuous eruptive activity over at least the past 15 years. The escape flux of water from Enceladus' plume calculated from our measurement of the column density may or may not represent steady state since the observation history is confined to a single flyby. Based simply on source magnitude however it is probable that

Enceladus is the dominant source of the observed neutral water product gas in the Saturn system.

The maintenance of the E-ring is also addressed by the UVIS observations although only the abundance of water vapor in the plume is determined by the occultation. A first order calculation of rate processes indicates that H<sub>2</sub>O gas alone falls short as a maintenance process against the calculated particle erosion rates. If Enceladus is a significant source for maintaining the E-ring it implies that grain particles be part of the mix of matter in the plume. If Enceladus' plume has a comet-like dust-to-gas mass ratio, the mass of water coming from Enceladus, >150 kg/sec, is more than sufficient to replace the estimated loss rate of the E ring of 1 kg/sec (22). The polar plume at Enceladus is clearly a uniquely important geophysical phenomenon.

### **References and Notes**

1. Smith, B. A. *et al.*, *Science* 215:504-536 (1982).
2. Showalter, M. R., J. N. Cuzzi, S. M. Larson, *Icarus* 94:451-473 (1991).
3. Terrile, R.J. and A. Cook, *Lunar Planet. Sci (Suppl. A)* 12:10 (1981).
4. Buratti, B. J., *Icarus* 75:113-126 (1988).
5. Horanyi, M., J. A. Burns, D. P. Hamilton, *Icarus* 97:248-259 (1992).
6. Esposito, L. *et al*, *Space Science Reviews* 115:299-361 (2004).
7. Dougherty, M. K. *et al.*, this issue.
8. Saur, J. and D. F. Strobel, *Astrophys. J.* 620:L115-L118 (2005).



9. Smith, G. R. and D. M. Hunten, *Rev. Geophys.* 28, 2:117-143 (1990).
10. Chan, W. F., G. Cooper, C. E. Brion, *Chem. Phys.*, 178:387-400 (1993).
11. Harreveldt, R. and M. C. Hemert, *JCP* 114:9453 (2001).
12. Waite, H. *et al.*, this issue.
13. Eidelsberg, M., F. Rostas, J. Breton, and B. Thieblemont, *J. Chem. Phys.* 96:5585-5590 (1992).
14. Spencer, J. *et al.*, this issue.
15. Nicholson, P. D., *et al.*, *Science* 272:509 (1996).
16. Jurac, S., R. E. Johnson, J. D. Richardson, *Icarus* 149:384-396 (2001).
17. Shemansky, D. P. Matheson, D. T. Hall, H.-Y. Hu and T. M. Tripp, *Nature* 363:329-331 (1993).
18. Esposito, L W., *et al.*, *Science* 307:1251-1255 (2005).
19. Jurac, S., M. A. McGrath, R. E. Johnson, J. D. Richardson, V. M. Vasyliunas, and A. Eviatar, *GRL* 29:2172 (2002).
20. Jurac, S. and J. D. Richardson, *JGR* 110:A09220 (2005).
21. Shemansky, D., L. Esposito and the Cassini UVIS team, *AGU abstract*, 2004.
22. Juhasz, A. and M. Horanyi, *JGR* 107 A6 1066 (2002).

### **Acknowledgement**

This work was partially supported by the Jet Propulsion Laboratory, California Institute of Technology, under a contract with the National Aeronautics and Space Administration.

We thank Nathan Strange for his efforts in ensuring that the gamma Orionis occultation was included in the design of Cassini's trajectory past Enceladus.

Table 1. Occultation geometry summary

<b>Occultation Date</b>		<b>Occultation intercept latitude</b>	<b>Occultation intercept longitude (west)</b>	<b>Atmosphere Detected?</b>
Feb. 17, 2005	Ingress	15	300	No
	Egress	-31	141	No
July 14, 2005	Ingress	-76	86	Yes
	Egress	-0.20	28	No

## Figure Captions

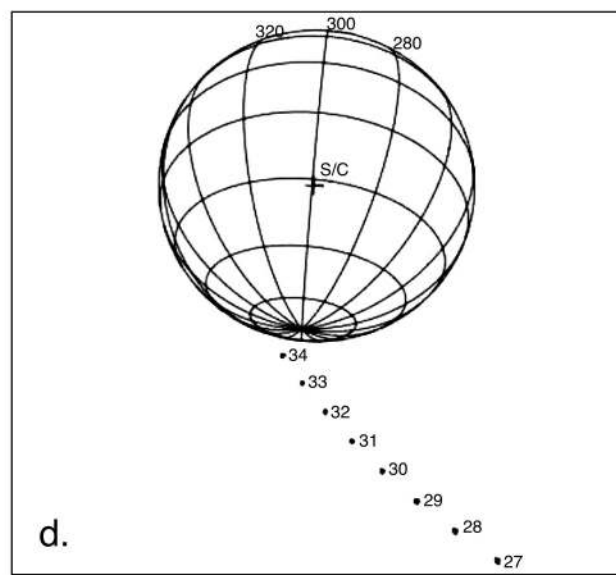
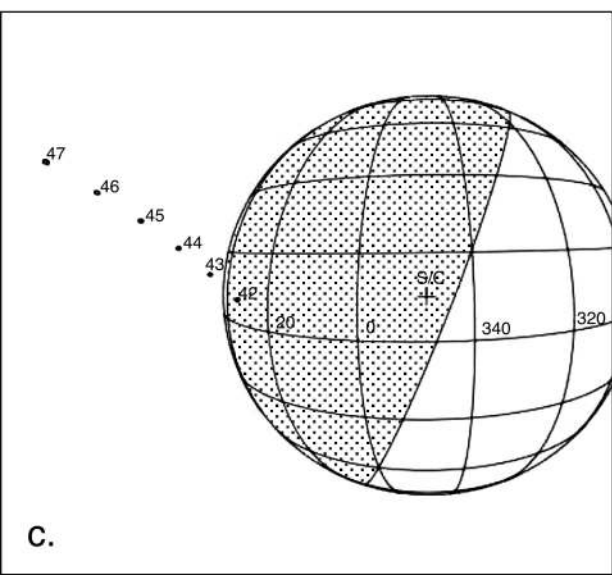
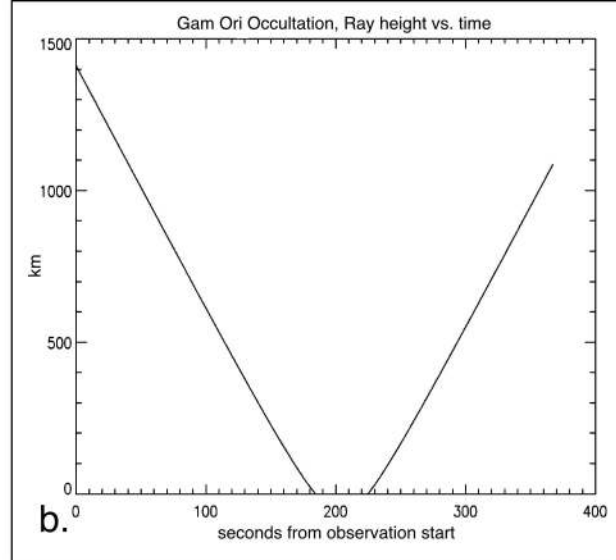
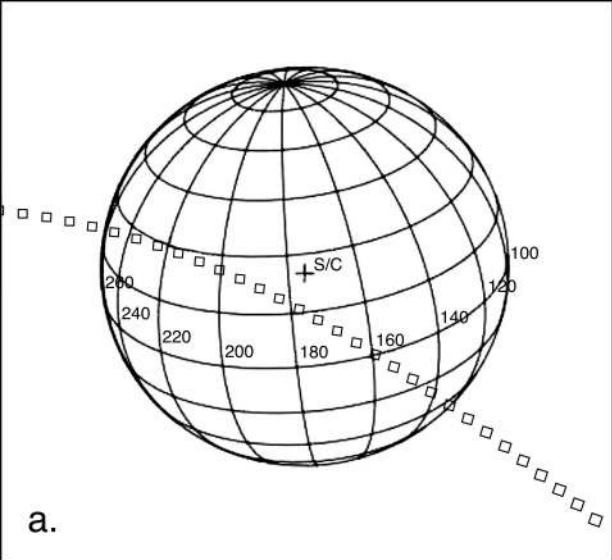
**Figure 1.** Frame **a** shows the path followed by the star lambda Scorpii as it was occulted by Enceladus, the first occultation observed by UVIS. The second stellar occultation observed was the star gamma Orionis. The altitude of the ray between the UVIS and the star relative to the surface of Enceladus is given in km as a function of time in Frame **b**. The path of gamma Orionis goes from right to left as a function of time, in frames **c** and **d**. Frame **d** illustrates the ingress of gamma Orionis, while **c** illustrates the egress. The UVIS field of view is plotted every 5 sec. The number over the field of view is the time record number of the data set.

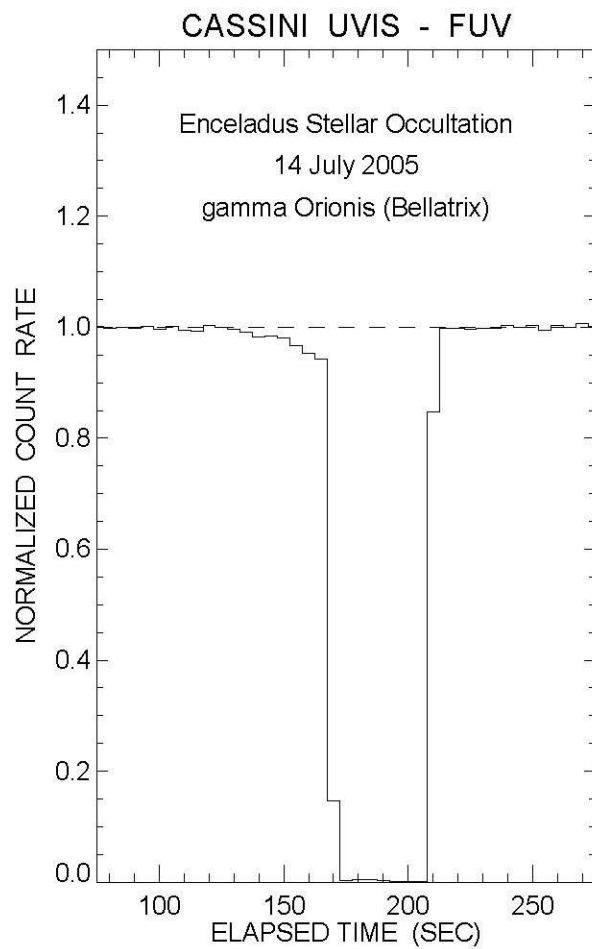
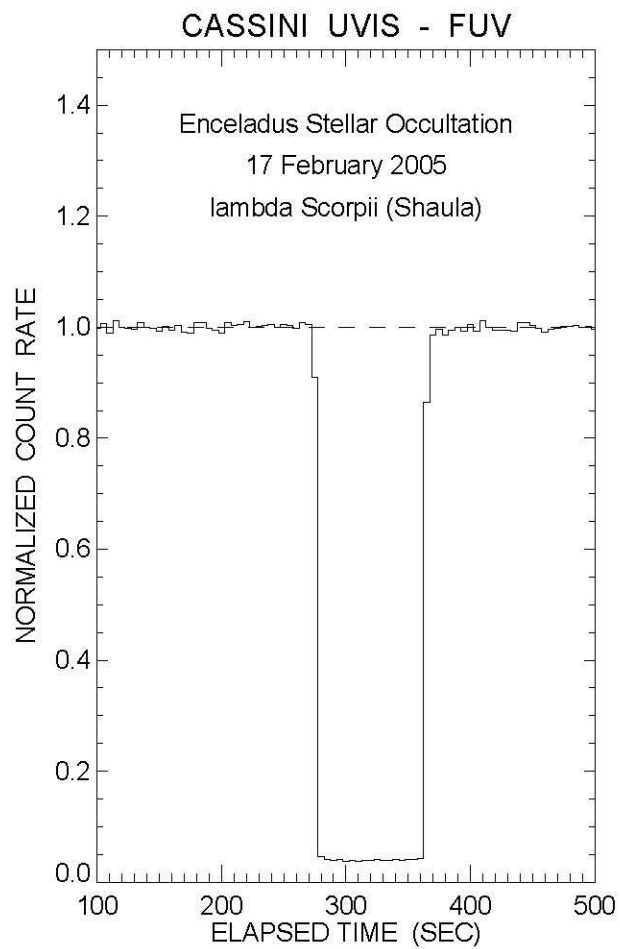
**Figure 2.** The signal of the star is plotted vs. time for the two occultations observed by UVIS. The left frame shows the steep drop in the FUV count rate as the star lambda Scorpii went behind the Enceladus, then re-emerged. Similarly the right frame shows the FUV data from the gamma Orionis occultation. The gradual drop of the signal during ingress is due to the starlight being attenuated by Enceladus' plume. Small steps in signal on both stars' ingress and egress correspond to the records in which the star was not in the FUV field of view (coming in and/or out of occultation) for the full 5 sec integration.

**Figure 3.** Smoothed FUV spectra are shown for the unocculted star signal (blue) compared to the signal coming through the plume (red).

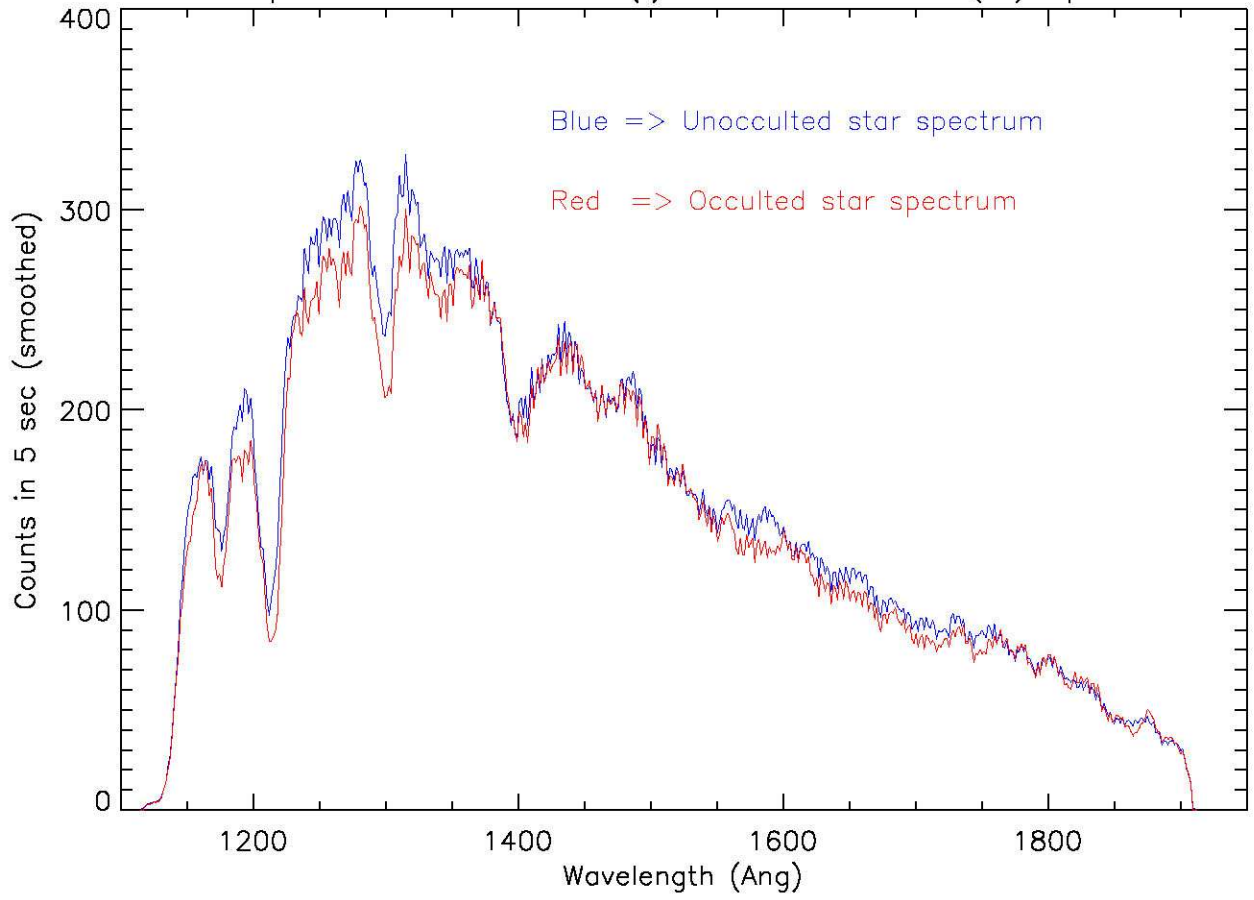
**Figure 4.** An average unocculted star spectrum ( $I_0$ ) was computed from 25 time records. The ratio of time record 33 ( $I$ ) to  $I_0$  is shown (thin line). A water spectrum with column density  $n = 1.5 \times 10^{16} \text{ cm}^{-2}$  divided by  $I_0$  is compared (thick line).

**Figure 5.** Water abundance is shown as a function of time (ticks are every 10 seconds), labeled with the ray height in km at a few representative times.

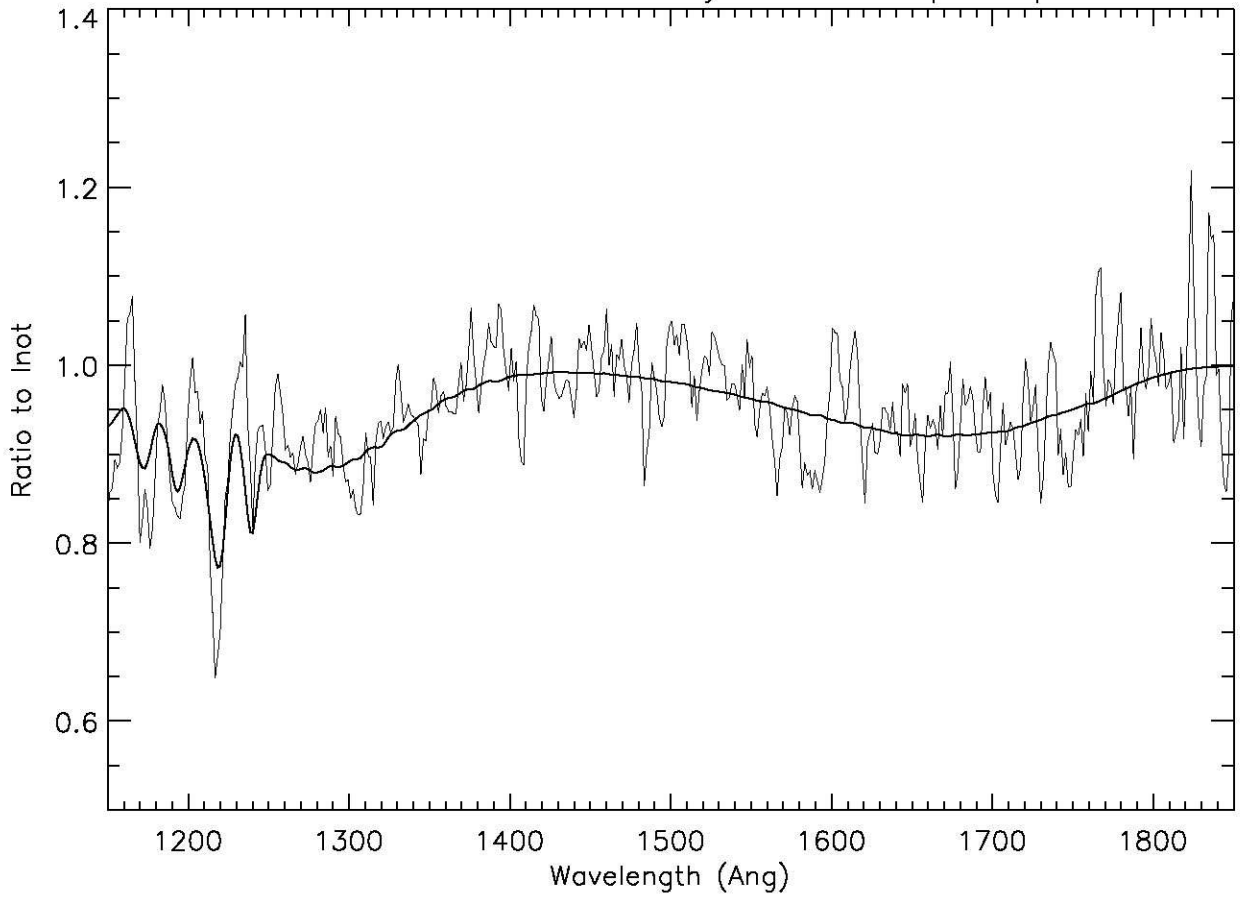




Comparison of occulted (I) and unocculted (Io) spectra



Water Fit for Column Density of  $1.5 \times 10^{16}$  per sq. cm





## CASSINI UVIS - ENCELADUS OCCULTATION

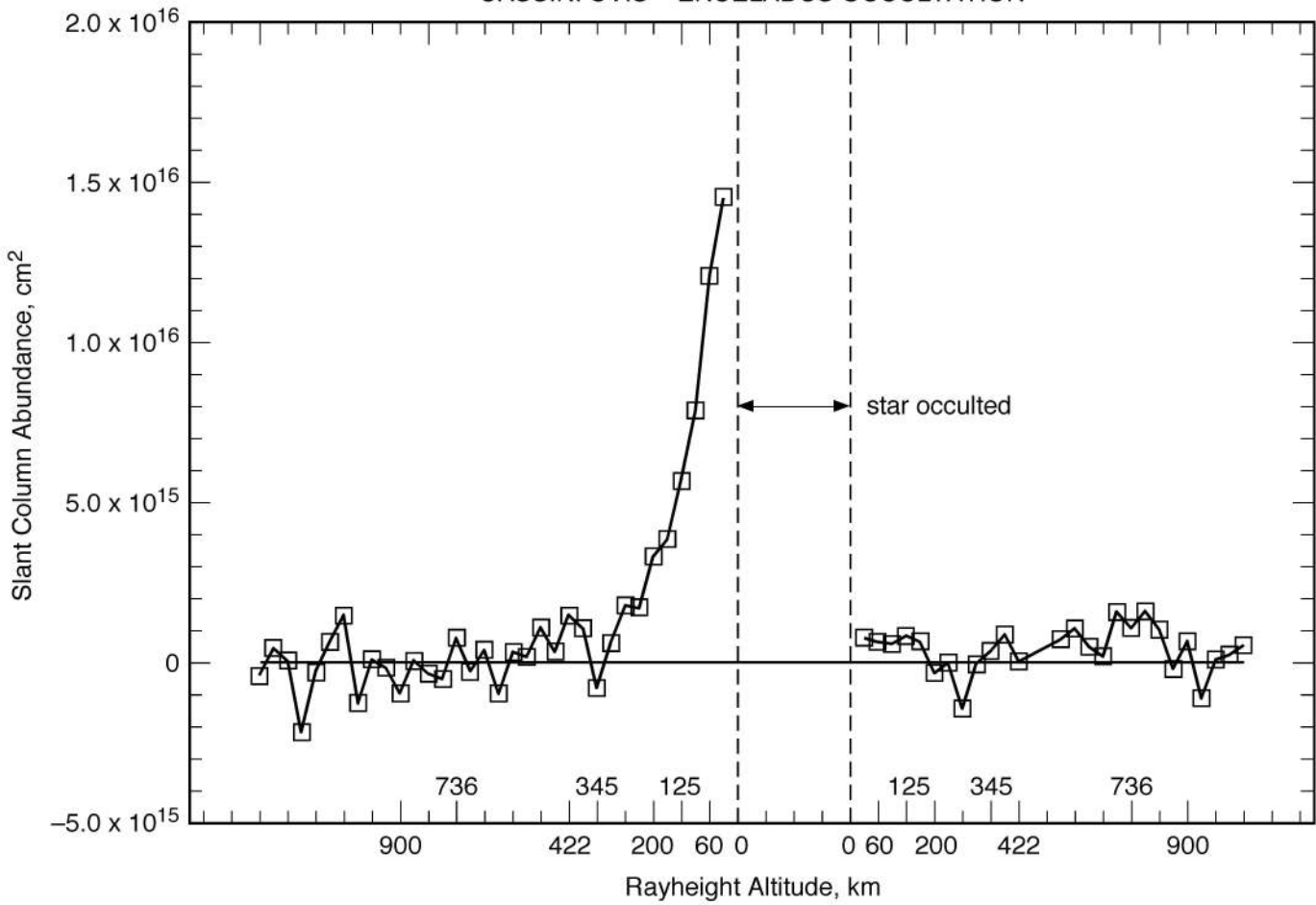


Figure 1 replacement for online issue of Science:

**Figure 1.** Frame **a** shows the path followed by the star lambda Scorpii as it was occulted by Enceladus, the first occultation observed by UVIS. The second stellar occultation observed was the star gamma Orionis. The path of gamma Orionis goes from right to left as a function of time, in frames **b** and **c**. Frame **c** illustrates the ingress of gamma Orionis, while **b** illustrates the egress. The altitude of the ray between the UVIS and the star relative to the surface of Enceladus is given in km as a function of time in Frame **d**. The UVIS field of view is plotted every 5 sec. The number over the field of view is the time record number of the data set. Frames **e** – **g** show the individual footprints and dramatic change in viewing geometry every 5 seconds as the star was occulted by Enceladus' plume.

